Proceedings of 2015 IEEE
International Conference on Mechatronics and Automation
August 2 - 5, Beijing, China

Temperature Characteristic of ring type dynamometer based on FBG sensors

Mingyao Liu , Zhijian Zhang, Dongliang Ji, Shuang Xiao
School of Mechanical and Electronic Engineering, Wuhan University of Technology, Wuhan 430070, China
Hubei Digital Manufacturing Key Laboratory, Wuhan 430070, China
E-mail: 1183030053@qq.com

Abstract - **In order to solve the problem that the measurement accuracy of FBG sensors used in the ring type dynamometer is vulnerable to be influenced by temperature fluctuations and others, a method for the temperature compensation of ring type dynamometer is necessary. A method that using wavelength multiplexed technology of fiber Bragg grating to test temperature and strain simultaneously has been proposed. This paper studies temperature characteristics of FBG sensors and annulus elastic body. Temperature calibration experiment which is used to obtain the temperature characteristic function of FBG sensors and annulus elastic body has also been done. Through the analysis of data, the temperature characteristic of ring type dynamometer has been obtained, and it owns good linearity. By using the temperature characteristic of ring type dynamometer, the effect of temperature fluctuation on the measurement accuracy can be compensated, which can enhance the cutting force measurement precision of ring type dynamometer.**

Keywords - Cutting Force, Ring Type Dynamometer, Temperature Characteristic, Temperature Calibration.

I. INTRODUCTION

Metal cutting is widely used in various industries, such as automotive, watercraft and project machine. During metal cutting, in order to prolong machine tool life and prevent tool breakage, mechanical properties of the milling tool should be known and therefore care should be taken to prevent this [1]. Cutting forces are one of the most important mechanical properties of machine tools, and they can be used to judge the operation state of machine tool. Knowledge of cutting forces is important in metal cutting, because it is also used as an important indicator in designing a machine tool, and used for cutting process optimization [2], investigation of the fundamental study of cutting tools performance, prediction of surface roughness, tool wear monitoring [3], machining process planning [4-5] and others.

Many studies have been conducted to obtain the values of cutting forces accurately. In the field of cutting force measurement, studies mainly focus on direct measurement of cutting force that using resistance strain gauge [1, 6-9] or piezoelectric element [10-12] to obtain the value of cutting forces. Resistance strain gage possesses high sensitivity, small volume, easy installation, low cost and other merits; however, it also has the demerits of complex line, wiring difficulty and easily being affected by interference factors. The main advantages of piezoelectric element are good rigidity, small volume and quick response, but it is very sensitive to temperature changes, humidity and electromagnetic disturbance, and the piezoelectric element itself has hysteresis characteristics, which cannot meet the cutting force test requirement. Fiber Bragg Grating (FBG) sensors, as optical sensor, are light in weight, small in volume, high in precision, immune to electromagnetic, resistant to corrosion and resistant to high temperature. Besides, it is easy to conduct distributed dynamic measurement. These characteristics, which many other types of sensors do not have, are suitable for machine tool condition monitoring and cutting force measurement, especially multiple FBG sensors used to test different or same parameters can be written on a single optical fiber which can achieve temperature, strain and a plurality of cutting force elements to be detected at the same time. Ref. [13] uses FBG sensors to measure cutting force; however the FBG sensors are directly pasted on the toolbar of turning tool which is easily influenced by cutting heat. For the sake of improving the accuracy of cutting force measurement, research group of machine tool of Wuhan University of Technology has developed a dynamometer based on FBG sensor and octagonal ring [14]. Due to the limitation of measurement sensitivity of octagonal ring, a new method that using FBG and annulus elastic body to measure the cutting force has also been developed [15].

Work pieces, especially precision and large work pieces, need a long time to be processed. During this period, the temperature of the environment will have certain fluctuation, and the machining process will produce a large number of cutting heat, so FBG sensors will be influenced by temperature fluctuation which will affect the accuracy of cutting force measurement. What's more, under the effect of temperature, annulus elastic body which is the basic force measuring element of ring type dynamometer will also produce thermal deformation. After thermal deformation, annulus will stretch or compress FBG sensors located in the interior of annulus, so it will make the reflected center wavelength of FBG sensors changed.

For the purpose of improving the measurement accuracy of annulus elastic body and removing the temperature interference factor on FBG sensors and annulus elastic body, a new method that using wavelength multiplexed technology of fiber Bragg grating to test temperature and strain at the same time has been proposed. The temperature characteristics of FBG sensors and annulus elastic body have been studied in this paper. Besides,

978-1-4799-7096-4/15/$31.00 ©2015 IEEE

the temperature calibration of annulus elastic body and FBG sensors has also been done, and the function between temperature and reflected center wavelength of FBG sensors has been obtained. We can realize the temperature compensation for annulus elastic body and solve the influence of temperature on the measurement precision of the cutting force, and improve the precision of cutting force measurement by using temperature characteristics.

II. RING TYPE DYNAMOMETER

A. Annulus diameter change rule

When the radius R of the annulus far outweighs its thickness h, in order to simplify the calculation, it can be simplified as a thin ring. Under the action of external loads, deformation of ring is shown in Figure 1.

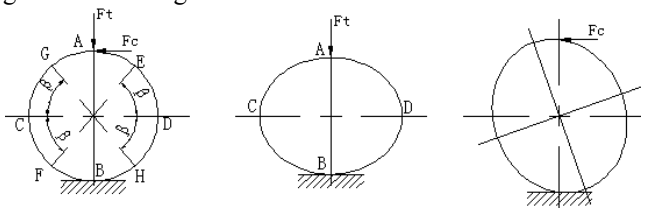

Fig 1. Deformation of ring under external forces

According to the knowledge of mechanics material and the related parameters of the annulus that are radius R, elastic modulus E, width h, thickness b and moment of inertia I, the relative displacement between two points located on the same diameter of one ring can be figured out.

The relative displacement between two points C and D is as follows:

$$\delta_{CD}=0.1369F_t\frac{R^3}{EI} \tag{1}$$

Where $I=bh^3/12$ is the moment of inertia of annulus elastic body.

The relative displacement between points E and F can be expressed in the following equation:

$$\delta_{EF}=(0.0334F_t-0.2802F_c)\frac{R^3}{EI} \tag{2}$$

The relative displacement between points G and H can be calculated as follows:

$$\delta_{GH}=(0.0334F_t+1.0795F_c)\frac{R^3}{EI} \tag{3}$$

By using formula (1), (2) and (3), the strain between points C and D, E and F, G and H can be figured out.

$$\varepsilon_{CD}=0.1369F_t\frac{R^3}{EIl_{CD}} \tag{4}$$

$$\varepsilon_{EF}=(0.0334F_t-0.2802F_c)\frac{R^3}{EIl_{EF}} \tag{5}$$

$$\varepsilon_{GH}=(0.0334F_t+1.0795F_c)\frac{R^3}{EIl_{GH}} \tag{6}$$

Where l_{CD} is the length of bare fiber between points C and D, l_{EF} is the length of bare fiber between points E and F, l_{GH} is the length of bare fiber between points G and H.

B. Annulus dynamometer of FBG

The diameter and cross sectional area of Optical fiber is just $0.125mm$ and $4.866\times10^{-2}mm^2$, so the contact between annulus elastic body and Optical fiber can be regarded as a point connection. In order to measure the relative displacement between two points located on the same diameter of one ring, the sensors FBG1, FBG2, FBG3 must be placed in the annulus between strain nodes C and D, E and F, G and H, and other kinds of sensor is difficult to test strain or relative displacement between two points. Besides, the FBG sensors should be preloaded to ensure they can measure the strain when annulus is compressed. For applying preload on the FBG and preventing rotation of FBG during pre-stressing, the pre-tightening device, which consists of fine adjustment nut, snap ring and slider, is also needed. On the basis of the above requirement, the basic structure of annulus elastic body has been designed as shown in Figure 2.

Through analyzing the sensitivity, static stiffness and natural frequency of the annulus elastic body, the static stiffness is proportional to bh^3/R^3 and the natural frequency is proportional to $\sqrt{bh^3/R^3}$, but the sensitivity is inversely proportional to bh^3/R^3. Therefore, in order to meet the condition of the static stiffness and natural frequency, the annulus elastic body should choose the larger R/h and smaller b to get high sensitivity. As a consequence, the annulus in this test chooses the radius R = 28 mm, height h = 7 mm, and width b = 25 mm.

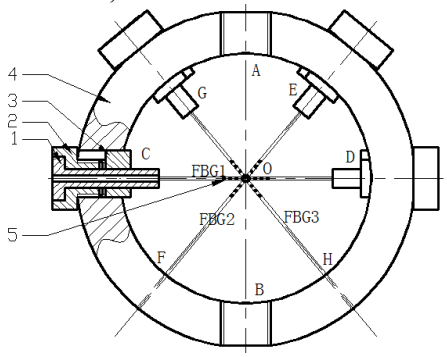

1. Slider; 2. Fine Adjustment Nut; 3. Snap Ring; 4. Annulus elastic body; 5. FBG

Fig 2. Annulus elastic body

C. Strain measurement principle of FBG sensor

The reflected center wavelength of grating λ_B mainly depends on the grating period Λ and its effective refractive index n_{eff}, and it can be figured out as follows:

$$\lambda_B=2n_{eff}\Lambda \tag{7}$$

When the strain or temperature applied on the Fiber Bragg grating change, effective refractive index and the fiber period of fiber grating will also change. The wavelength of light that being reflected by grating will change from λ_{B_0} to λ_B, so it can be considered as a function of strain σ and temperature T, and its change can be calculated as follows:

$$\Delta\lambda_B=\lambda_B(\sigma,\mathrm{T})-\lambda_{B_0}(\sigma_0,\mathrm{T}_0) \tag{8}$$

Where λ_{B_0} is the reflected center wavelength of grating before the strain or temperature applied on the Fiber Bragg

grating occur change; σ_0 is initial strain applied on the Fiber Bragg grating; T_0 is initial temperature applied on the Fiber Bragg grating.

Make the formula (7) as a Taylor expansion and take the first order approximation, and pull in Young's modulus of fiber Y_F, thermal expansion coefficient α_Λ, thermo-optic coefficient α_n and photo elasticity coefficient P_e, then the wavelength shift can be expressed in the following equation:

$$\Delta\lambda_B = \lambda_{B_0}[(1-P_e)\Delta\varepsilon + (\alpha_\Lambda + \alpha_n)\Delta T] \quad (9)$$

Where $\Delta\varepsilon$ represents the variation of axial strain of Optical fiber; ΔT represents the change of temperature, which is equal to $\Delta\sigma / Y_F$; $\Delta\sigma$ represents the change of axial stress of Optical fiber.

Once we get the strain between points C and D, E and F, G and H, by using formula (4), (5) and (6), the value of external forces can be calculated out, and the direction of forces can also be judged out. Type (9) shows that both strain and temperature have an effect on the change of wavelength. For the sake of getting strain value tested by FBG sensor, the wavelength variation incurred by temperature fluctuation must be removed.

III. Research of Temperature Characteristic

A. Temperature characteristic of FBG sensor

The fluctuation of ambient temperature can cause the thermal expansion effect and thermo-optic effect of fiber-optical change which will finally lead to the reflected wavelength of grating change [16]. The equation (7) tells that the Bragg wavelength changes along with the effective refractive index and lattice spacing. When the environment temperature around the grating changes, fiber Bragg grating temperature changes as well. Due to the thermo-optic effect of fiber materials, grating effective refractive index changes along with the temperature; thermal deformation of fiber material makes the lattice spacing of the grating change, all of these results in reflection wavelength of the grating drift. The derivative with respect to temperature in equation (7) can get the temperature change function of the grating:

$$d\lambda_B / dT = 2(n_{eff} d\Lambda / dT + \Lambda dn_{eff} / dT) \quad (10)$$

Changes of the grating period caused by thermal expansion effect can be expressed in the following equation:

$$d\Lambda / dT = \alpha_\Lambda \cdot \Lambda \quad (11)$$

The effective refractive index change caused by thermo-optic effect is shown as follows:

$$dn_{eff} / dT = n_{eff} \cdot \alpha_n \quad (12)$$

By using formulas (7), (10), (11) and (12), the temperature change function of the grating can be obtained by using the follow relation:

$$d\lambda_B = \lambda_{B_0} \cdot (\alpha_\Lambda + \alpha_n)\,\mathrm{dT} \quad (13)$$

Integrating the both sides in the type (10) gets the following equation:

$$\lambda_{B_T} = \lambda_{B_0} K_T T + C \quad (14)$$

Where $K_T = \alpha_\Lambda + \alpha_n$ is temperature sensitivity of fiber-optical.

From type (14), reflection wavelength of grating changing with the temperature fluctuations is linear. For quartz optical fiber, the thermal expansion coefficient is $\alpha_\Lambda \approx 0.5\times10^{-6}/^\circ\mathrm{C}$, thermo-optical coefficient is $\alpha_n \approx 6.7\times10^{-6}/^\circ\mathrm{C}$ [17], so the temperature sensitivity of quartz optical fiber is about $7.2\times10^{-6}/^\circ\mathrm{C}$. For $1500pm$ series of quartz optical fiber, grating wavelength drift caused by the temperature variation is about $1500\times7.2\times10^{-6} = 0.0108nm$, it is $0.0108nm/^\circ C$.

From formula (9) we can see that the data detected by FBG sensor contains strain and temperature. For a sensor, when multiple factors have effect on the output signal at the same time, the cross sensitivity should be considered. However, for FBG sensors, when the range of temperature change is within 100 degree Celsius, we can ignore the cross sensitivity of strain and temperature [16]. That means strain and temperature effect on the optical fiber grating can be regarded as independent. After ignoring the influence of cross sensitivity, the wavelength shift caused by strain and temperature can be expressed in the following equation:

$$\Delta\lambda_\mathrm{B} = (\mathrm{K}_T + \mathrm{K}_\varepsilon)\cdot\lambda_{\mathrm{B}_0} \quad (15)$$

Where $K_T = 1 - P_e$ is strain sensitivity of fiber-optical.

Once we got the wavelength shift caused by temperature, we can get the real strain measured by FBG sensors as follows:

$$\Delta\lambda_{\mathrm{B}\varepsilon} = \Delta\lambda_\mathrm{B} - \Delta\lambda_{\mathrm{B}T} \quad (16)$$

Where $\Delta\lambda_{\mathrm{B}\varepsilon} = K_\varepsilon \cdot \lambda_{\mathrm{B}_0}$ is the wavelength shift caused by strain; $\Delta\lambda_{\mathrm{B}T} = K_T \cdot \lambda_{\mathrm{B}_0}$ is the wavelength shift caused by temperature fluctuation.

B. Temperature characteristic of annulus elastic body

When the temperature change, annulus elastic body will produce thermal deformation which will lead to FBG sensors fitted in annulus being stretched or compressed. For obtaining the thermal deformation rule of annulus, the finite element analysis of annulus has been done. In order to simplify the calculation, we just use simplified annulus to analysis. The temperature we set is $25^\circ C$, $35^\circ C$, $45^\circ C$, $55^\circ C$ and $65^\circ C$ respectively, the thermal deformation of two strain nodes located at one diameter is $0.97364\mu m$, $4.21874\mu m$, $7.46384\mu m$, $10.70894\mu m$ and $13.95404\mu m$ respectively, the relation curve between temperature and displacement after thermal deformation is shown in Figure 3. We can get the conclusion that the relationship between temperature and thermal deformation is linear.

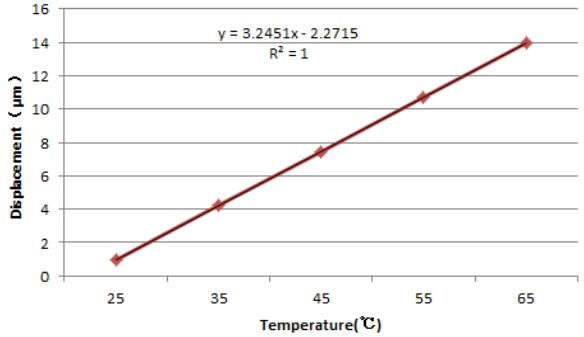

Fig. 3. Relation between temperature and displacement after thermal deformation

IV. TEMPERATURE CALIBRATION

A. Temperature calibration of FBG sensor

There are three FBG sensors in each annulus elastic body namely FBG 1, FBG 2 and FBG 3, as shown in Figure 2. FBG 1 located between points C and D is used to measure ε_{CD}; FBG 2 located between points E and F is used to measure ε_{EF}; FBG 3 located between points G and H is used to measure ε_{GH}. However, the output data not only contains cutting force, but also includes temperature. In order to remove the temperature data from the output data and realize synchronous temperature compensation, FBG 4 which is just used to measure temperature in the process of machining is needed. As the doping elements and doping concentration of optical fiber are subtle differences, the temperature characteristic of FBG sensor is not completely consistent with theoretical calculation. In order to get the temperature characteristic of FBG sensor, we need to calibrate the temperature characteristics of FBG sensor.

Before calibration, FBG sensors (FBG 1, FBG 2, FBG 3 and FBG 4), optical demodulator, computer, thermometer and vacuum flask should be composed into a temperature calibration system, as shown in Figure 4. The thermometer used for measuring the water temperature in vacuum flask is second class mercury thermometer, and the temperature measurement accuracy of it is $0.1^{\circ}C$. The decrease value of water temperature in vacuum flask which is used to ensure the water temperature constant is only $0.1^{\circ}C$ per hour [18]. Owing to the time used for recording the water temperature value and wavelength value of FBG sensors is far less than one hour, the water temperature can be regarded as a constant value during experiment operation. In the process of temperature calibration, we should regulate vacuum flask to keep the water temperature at a predetermined value, and then record the Bragg wavelength value and the water temperature value simultaneously when water temperature is stable. Then, gradually change the temperature of water to finish temperature calibration. The Bragg wavelength value and the temperature value of water are fitted by least square method, by which we can get the temperature characteristic of FBG sensors, as shown in Figure 5.

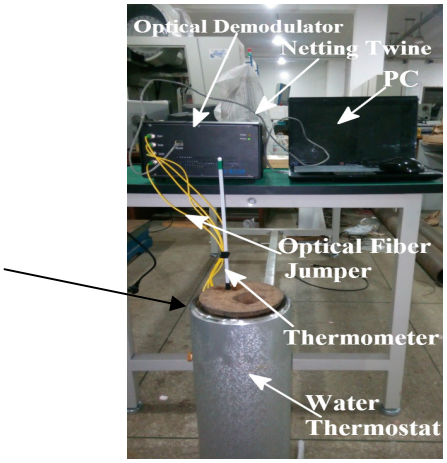

Fig 4. Temperature Calibration System with Water Thermostat

Figure 5 shows that the grating wavelength drift of FBG 1, FBG 2 and FBG 3 before installed in the annulus elastic body and FBG 4 caused by the unit temperature variation are $0.01082\,\text{nm}/^{\circ}\text{C}$, $0.01085\,\text{nm}/^{\circ}\text{C}$, $0.01094\,\text{nm}/^{\circ}\text{C}$ and $0.01073\,\text{nm}/^{\circ}\text{C}$ respectively. The error between the experimental data and theoretical calculation value are 0.185%, 0.463%, 1.329% and 0.648% respectively. From this we can certify that the theoretical value is not completely consistent with the test data, but the difference is very small. The linear fitting of FBG 1, FBG 2, FBG 3 and FBG 4 are 0.9996, 0.9994, 0.9991 and 0.9996 respectively, so FBG sensors own good linearity, and it can be used to test the temperature fluctuation during the machining process. Owing to the resolution of optical fiber demodulator is $1pm$, so the sensitivity of FBG 4 which is used to measure the temperature is 0.093°C.

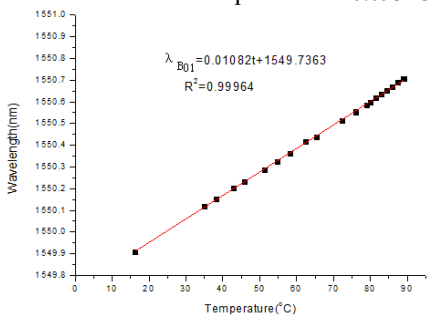

FBG 1

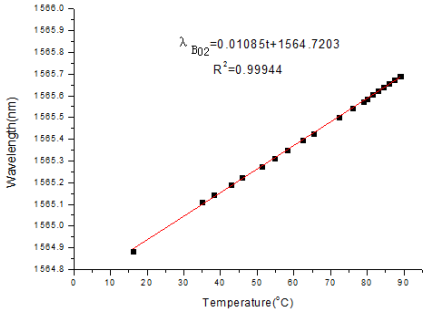

FBG 2

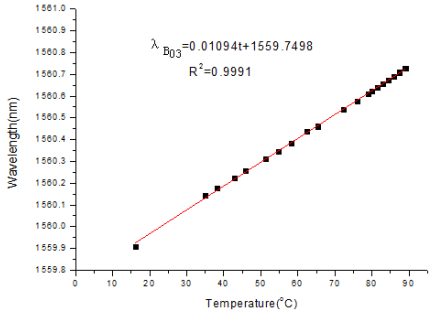

FBG 3

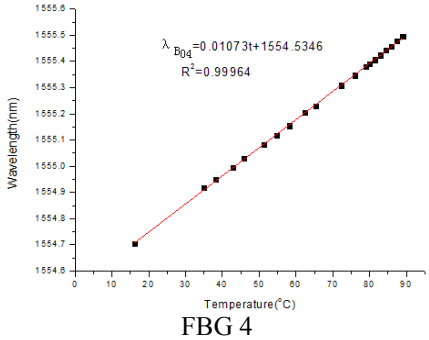

FBG 4

Fig 5. Temperature Characteristic of FBG

B. Temperature calibration of Ring type dynamometer

The output data of the three FBG sensors located in the annulus which are used to measure the cutting force not only contains cutting force, but also includes temperature. Temperature has direct influence on FBG sensors; besides, the thermo deformation of annulus elastic body can stretch or compress FBG sensor which will also cause the wavelength change of FBG sensors. In order to remove the temperature data from the output data and realize synchronous temperature compensation, the effect of thermo deformation of annulus elastic body on FBG1, FBG 2 and FBG 3 fitted in the annulus must be obtained. Then we can use the temperature measured by FBG 4 in the process of machining to get the wavelength shift of FBG1, FBG 2 and FBg3 caused by temperature fluctuation during machining process.

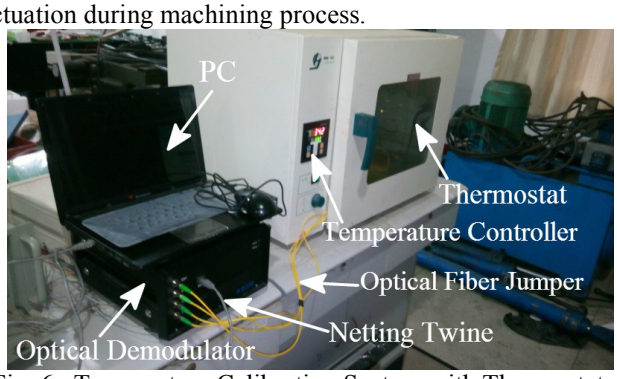

Fig. 6. Temperature Calibration System with Thermostat

Annulus elastic body cannot be put into vacuum flask, so thermostat is utilized to replace thermometer and vacuum flask in temperature calibration system, as shown in the Figure 6. In order to obtain the temperature characteristic of annulus elastic body, the annulus elastic body and FBG 4 need to be put into the thermostat together. What's more, they should be placed at the same place as far as possible to ensure the temperature around them is identical. Adjust the initial temperature of the thermostat higher than ambient temperature and store the Bragg wavelength value and the temperature value of thermostat when the temperature becomes stable. Raise the temperature of the thermostat step by step and read the data when the temperature becomes stable in each step.

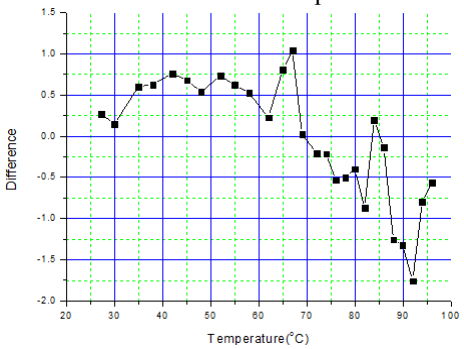

Fig. 7. Difference between temperature shown in thermostat and the temperature measured by FBG sensor

The model number of the thermostat used in this study is Jing Hong XMTD-8222 and its error of temperature is $\pm 2^{\circ}C$ which is a larger than FBG 4, so we use the data measured by FBG4 and its temperature characteristic to calculate the actual temperature rather than the temperature shown in thermostat. The difference between temperature shown in thermostat and temperature measured by FBG 4 is shown in Figure 7. The difference shown in Figure 7 is comply with the error of temperature of thermostat, so we use the calculated temperature to get the linear fitting of FBG 1, FBG 2 and FBG 3 located in the annulus elastic body and FBG 4, as shown in the Figure 8.

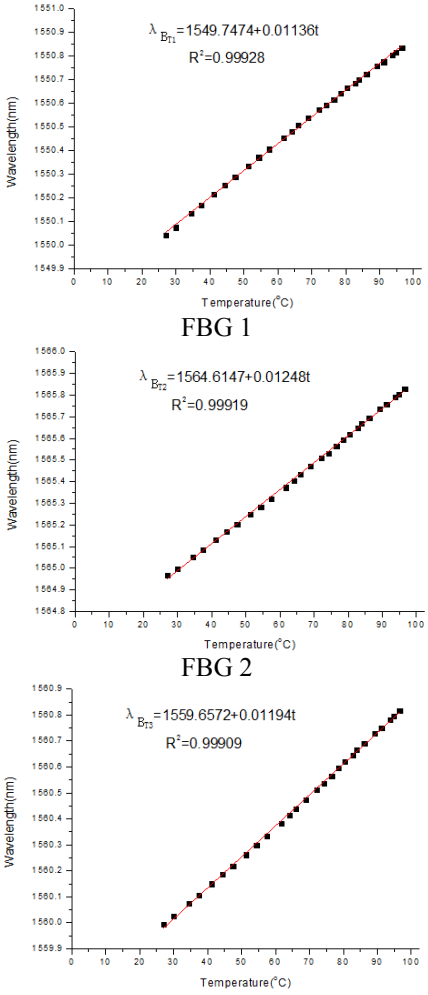

Fig. 8. Temperature characteristic of FBG located in Annulus

From Figure 8, we can know that the wavelength shift caused by the unit temperature variation of FBG 1,FBG 2 and FBG 3 fitted in the annulus is $0.01136nm/°C$, $0.01248nm/°C$ and $0.01194nm/°C$ respectively. Compared with the intrinsic temperature characteristic of FBG sensors, under the influence of thermo deformation of annulus elastic body, the wavelength shift caused by the unit temperature variation of FBG sensors has increased 4.99% 、 15.02% and 9.14% respectively. According to the result, the influence of wavelength shift impacted by thermal deformation of annulus cannot be ignored. The linearity of the fitted curve of FBG 1, FBG 2 and FBG 3 fitted in the annulus is 0.99928, 0.99919 and 0.99909 respectively, and the linearity is very high. Besides, compared with intrinsic temperature characteristic of FBG sensors, the linearity of FBG 1, FBG 2 and FBG 3 has only fallen 0.036% , 0.025% and 0.001% respectively. The thermal deformation of the ring can be regarded as vary linearly with temperature fluctuation, and it comply with theoretical analysis.

The temperature characteristic function of FBG 1, FBG 2 and FBG 3 located in annulus is as follows.

$$\begin{cases} \lambda_{B_{T1}} = 0.01136t + 1549.7474 \\ \lambda_{B_{T2}} = 0.01248t + 1549.6147 \\ \lambda_{B_{T3}} = 0.01194t + 1559.6572 \end{cases} \quad (17)$$

During cutting force measurement, FBG 4 can measure the temperature change. By using formula (16) and (17), we can realize temperature compensation and get the real stain measured by FBG sensors.

V. CONCLUSION

In this paper, the principle of FBG sensor measuring temperature and strain has been studied, and a method that using the temperature characteristic of FBG to realize temperature compensation has been proposed. In order to get the temperature characteristic of annulus elastic body, the finite element analysis of annulus has also been done and the relationship between temperature and annulus deformation has been obtained. Besides, the temperature calibration of FBG sensors and annulus elastic body has been done and the function between temperature and reflected wavelength has been gotten. The real-time data of temperature change during machining process can be gathered by using FBG temperature sensor, and then it can be used for temperature compensation of cutting force which can improve the precision of cutting force measurement.

ACKNOWLEDGMENT

This experimental study was supported by the National Natural Science Fund of Chinese (General Program, Grant NO51375359) and Independent Innovation Foundation of Wuhan University of Technology (Grant NO145204010). The authors would like to thank Hubei Digital Manufacturing Key Laboratory (Wuhan University of Technology) for providing experiment equipment to accomplish the project.

REFERENCES

[1] Ihsan Korkut, "A dynamometer design and its construction for milling operation," Materials & design, 24, pp. 631-637, Dec. 2003.

[2] F. Cus, M. Milfelner, J. Balic, "An intelligent system for monitoring and optimization of ball-end milling process," Journal of Materials Processing Technology, 175, pp. 90-97, Jun, 2006.

[3] Zuperl Uros, Cus Franc, Kiker Edi, "Adaptive network based inference system for estimation of flank wear in end-milling," Journal of Materials Processing Technology, 209, pp. 1504-1511, Feb, 2009.

[4] Baohai Wu, Xue Yan, Ming Luo, Ge Gao, "Cutting force prediction for circular end milling process," Chinese Journal of Aeronautics, 26, pp.1057-1063, Aug, 2013.

[5] Han Xiong, Limin Tang, "Precise prediction of forces in milling circular corners," International Journal of Machine Tools and Manufacture, 88, pp. 184-193, Jan, 2015.

[6] Süleyman Yaldız, Faruk Ünsaçar, "Design, development and testing of a turning dynamometer for cutting force measurement," Materials & design, 27, pp.839-846, Jun. 2006.

[7] Sedat Karabay, "Analysis of drill dynamometer with octagonal ring type transducers for monitoring of cutting forces in drilling and allied process," Materials & design, 27, pp. 637-685, Aug. 2007.

[8] Süleyman Yaldiz, Faruk Ünsaçar, Haci Saglam, Hakan Isik, "Design, development and testing of a four-component milling dynamometer for the measurement of cutting force and torque," Mechanical Systems and Signal Processing, 21, pp. 1499-1511, Aug. 2006.

[9] Muhammad Rizal, Jaharah A. Ghani, Mohd Zaki Nuawi, Che Hassan Che Haron, "Development and testing of an integrated rotating dynamometer on tool holder for milling process," Mechanical systems and signal processing, 52, pp. 559-576, Aug. 2014.

[10] G. Totis, M. Sortino. "Development of a modular dynamometer for triaxial cutting force measurement in turning," International Journal of Machine Tools and Manufacture, 51, pp. 34-42, Oct. 2011.

[11] Lei Ma, Shreyes N. Melkote, John B. Morehouse, James B. Castle, James W. Fonda, Melissa A. Johnson, "Thin-film PVDF sensor-based monitoring of cutting forces in peripheral end milling," Journal of Dynamic Systems, Measurement, and Control, 134, pp. 05-14, Jul. 2012.

[12] F. Klocke, S. Gierlings, O. Adams, T. Auerbach, S. Kamps, D. Veselovac, M. Eckstein, A. Kirchheim, M. Blattner, R. Thiel, D. Kohler, "New concepts of force measurement systems for specific machining processes in aeronautic industry," Fifth CIRP Conference on High Performance Cutting, Zurich, 2012, pp. 5552-557.

[13] Liu Zhaoyan, Lei Zhenshan, "Measurement technique of cutting force by using fiber Bragg grating and virtual instrument," Tool Engineering, 39, pp. 53-56, Mar. 2005.

[14] Mingyao Liu, Zude Zhou, Xiaoliang Tao, Yuegang Tan, "A dynamometer design and analysis for measurement the cutting forces on turning based on optical fiber Bragg Grating sensor," Tenth World Congress on Intelligent Control and Automation, Beijing, 2012, pp. 4287-4290.

[15] Mingyao Liu, Zhijian Zhang, Zude Zhou, Shuang Peng, Yuegang Tan, "A new method based on Fiber Bragg grating sensor for the milling force measurement," to be published.

[16] Wei Cai. Study on FBG Temperature Sensing technology [D]. Wuhan: Wuhan University of Technology, 2004.

[17] Liao Yanbiao. Fiber Optics. China: Beijing, 2000, pp. 20-25.

[18] Erlong Zhang. Measurement of temperature field for the spindle of Machine tool based on Optical fiber Bragg grating sensors [D]. Wuhan: Wuhan University of Technology, 2014.